Journal of Solid State Chemistry 184 (2011) 164–170

Contents lists available at ScienceDirect

Journal of Solid State Chemistry

journal homepage: www.elsevier.com/locate/jssc

Crystal structures and luminescent properties of lanthanide nitrate coordination polymers with structurally related amide type bridging podands

Qing Wang, Xuhuan Yan, Hongrui Zhang, Weisheng Liu, Yu Tang *, Minyu Tan

Key Laboratory of Nonferrous Metal Chemistry and Resources Utilization of Gansu Province, State Key Laboratory of Applied Organic Chemistry, College of Chemistry and Chemical Engineering, Lanzhou University, Lanzhou 730000, PR China

ARTICLE INFO

Article history:
Received 13 July 2010
Received in revised form
15 October 2010
Accepted 8 November 2010
Available online 13 November 2010

Keywords:
Lanthanide
Coordination polymers
Podand
Luminescent properties

ABSTRACT

A one-dimensional linear chain coordination polymer $[ErL^{I}(NO_3)_3(CH_3CO_2Et)]_n$ (L^{I}=1,2-bis{[(2'-furfurylaminoformyl)phenoxyl]methyl}benzene) and a one-dimensional zig-zag coordination polymer $\{[TbL^{II}(NO_3)_3(H_2O)]\cdot(H_2O)\}_n$ (L^{II}=1,2-bis{[2'-(2-pyridylmethylaminoformyl)phenoxyl]methyl}benzene) were assembled by two structurally related bridging podands L^{I} and L^{II} which have uniform skeleton and different terminal groups. In $\{[TbL^{II}(NO_3)_3(H_2O)]\cdot(H_2O)\}_n$, the neutral chains were linked by the hydrogen bonding interactions between the free and coordinated water molecules from two different directions to interpenetrate into a 3D supramolecular structure. At the same time, the luminescent properties of the solid Tb(III) nitrate complexes of these podands were investigated at room temperature. The lowest triplet state energy levels T_1 of the podands L^{I} and L^{II} indicate that the triplet state energy levels of the antennae are both above the lowest excited resonance level of $^5D_4$ of Tb^{3+} ion. Thus the absorbed energy could be transferred from ligands to the central Tb^{3+} ions. And the influence of the hydrogen bonding on the luminescence efficiencies of the coordination polymers was also discussed.

1. Introduction

Lanthanide have been extensively employed in the metal directed synthesis in functional supramolecular structures and self-assemblies due to their unique luminescent, magnetic, and coordination properties [1–4]. The applications of the lanthanide complexes in luminescent sensing and imaging technology, and as contract agents for MRI are very well established [5–10]. Among the luminescent complexes studied, europium(III) and terbium(III) complexes appear to be the most attractive in view of the high photoluminescent (PL) efficiency and the narrow band red/green-emission ability, which may exploited in the full-color displays [11–14] and a variety of applications ranging from chemosensors for bioactive species to active components in time resolved assays. Since the *f–f* transitions are spin- and parity-forbidden, the design of efficient luminescent lanthanide(III) complexes continues to be an active area of research. The weak absorbance can be overcome by coordinating ligands containing chromophores to the lanthanide ion, which upon irradiation, transfers energy to the central metal ions, typically *via* the ligand triplet excited state, populating the lanthanide(III) emitting levels in a process known as the antenna effect [15–18].

Amide type podands have been attracting more attentions in preparing lanthanide complexes possessing strong luminescent properties. It is expected that the amide type podands which have flexible arms and "terminal-group effects" [19], will shield the encapsulated lanthanide ions from interaction with the surroundings effectively, and thus to have novel coordination structures and exhibit good luminescent properties. Our group has been interested in employing self-assembly strategies for luminescent lanthanide coordination polymers, and has recently used podands as sensitizers for lanthanide luminescence. As a part of our systematic studies, this work reports the assembly of two lanthanide coordination polymers including a one-dimensional (1D) linear chain coordination polymer $[ErL^{I}(NO_3)_3(CH_3CO_2Et)]_n$ and a one-dimensional (1D) zig-zag coordination polymer $\{[TbL^{II}(NO_3)_3(H_2O)]\cdot(H_2O)\}_n$ (L^{I}=1,2-bis{[(2′-furfurylaminoformyl)phenoxyl]methyl}benzene, L^{II}= 1,2-bis{[2'-(2-pyridylmethylaminoformyl)phenoxyl]methyl}benzene [20], Scheme 1) by two structurally related amide type bridging podands which have uniform skeleton and different terminal groups, and the luminescent properties of the Tb(III) complexes. The lowest triplet state energy levels of the two ligands which were calculated from the phosphorescence spectra of the Gd(III) complexes at 77 K indicate that the triplet state energy levels of the antennae are both above the lowest excited resonance level of $^5D_4$ (20,545 cm^{-1}) of Tb(III), and the absorbed energy could be transferred from podand L^{I} or L^{II} to the Tb(III). And the influence of the structures of the coordination polymers on the luminescent intensities of the complexes was also discussed.

* Corresponding author. Fax: +86 931 8912582.
E-mail address: tangyu@lzu.edu.cn (Y. Tang).

0022-4596/$ - see front matter © 2010 Elsevier Inc. All rights reserved.
doi:10.1016/j.jssc.2010.11.011

2. Experimental

2.1. Materials

Furfurylsalicylamide [21] were prepared according to the literature methods. The other commercially available chemicals were of A.R. grade and were used without further purification.

2.2. Methods

Carbon, nitrogen and hydrogen were determined on an Elementar Vario EL. Powder X-ray diffraction patterns (PXRD) were determined with Rigaku-Dmax 2400 diffractometer using Cu$K\alpha$ radiation. The FT-IR spectra were recorded on a Nicolet 360 FT-IR instrument using KBr disks in the 4000–400 cm^{-1} region. ^1H NMR spectra were measured on a Bruker AM400 spectrometer in *d*-chloroform solutions, with TMS as internal standard. Luminescence spectra and phosphorescence spectra were obtained on a Hitachi F-4500 fluorescence spectrophotometer. The quantum yields of the terbium samples were determined by an absolute method using an integrating sphere (150 mm diameter, $BaSO_4$ coating) from Edinburgh Instruments FLS920. The lifetime measurements were measured on an Edinburgh Instruments FLS920 Fluorescence Spectrometer with Nd pumped OPOlette laser as the excitation source. Reported luminescence lifetimes are averages of at least three independent determinations.

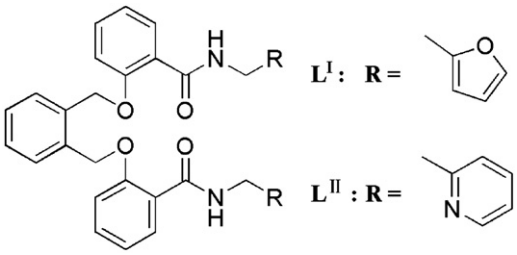

Scheme 1. The schematic illustration of the ligands L^I and L^{II}.

2.3. Crystal structure determination

Suitable single crystal of the nitrate complexes were carefully selected under an optical microscope and subsequently glued to the tip of a glass fiber. Intensity data were collected on a Bruker SMART 1000 CCD diffractometer using Mo$K\alpha$ radiation (λ=0.71073 Å) and integrated using the SAINT suite of software. The absorption corrections were calculated using SADABS. Primary non-hydrogen atoms were solved by direct method and refined anisotropically by full-matrix least-squares methods on F^2. Hydrogen atoms were placed in calculated positions and included in the final cycles of refinement using a riding model. The programs for structure solution and refinement were SHELXS-97 and SHELXL-97, respectively [22]. The crystal data and refinement results are summarized in Table 1, and selected bond lengths and angles are given in Tables 2 and 3 respectively. CCDC reference numbers 783278 and 783279.

2.4. Syntheses of the ligands

The podand 1,2-bis{[(2'-furfurylaminoformyl)phenoxyl]-methyl}benzene (L^I) was prepared by the following synthetic route. Furfurylsalicylamide [21] (7.5 mmol) and anhydrous potassium carbonate (8.1 mmol) were refluxed in acetone (50 cm^3) for 30 min, then the o-xylene dibromide (3.4 mmol) was added to the solution. The reaction mixture was refluxed for 12 h. After cooling down, the mixture was filtered and the solvent was distilled off. Then the resulted solid was recrystallized with acetone to get the ligand L^I; Yield: 81%; m.p.: 143–144 °C; ^1H NMR ($CDCl_3$, 400 MHz): 4.50(d, 4H), 5.15(s, 4H), 6.01(d, 2H), 6.21(d, 2H), 6.94(d, 2H), 7.06–7.48(m, 10H), 8.00(s, 2H), 8.21(t, 2H) ppm. IR (KBr, ν, cm^{-1}): 3386(m), 3062(m), 1639(s, C=O), 1600(m), 1537(s), 1299(s), 1245(s), 1115(m), 754(s), 695(m). Anal. Calcd. for $C_{32}H_{28}N_2O_6$ (%): C, 71.63; H, 5.26; N, 5.22; Found (%): C, 71.75; H, 5.16; N, 5.20.

Table 1
Crystal data and structure refinements for the Er(III) and Tb(III) complexes.

Empirical formula	$C_{36}H_{36}N_5O_{17}Er$	$C_{34}H_{34}N_7O_{15}Tb$
Formula weight	977.96	939.6
Temperature (K)	296(2)	296(2)
Wavelength (Å)	0.71073	0.71073
Crystal system, Space group	Triclinic, $P-1$	Orthorhombic, *Pbca*
a (Å)	11.7595(16)	17.818(4)
b (Å)	12.994(2)	17.818
c (Å)	13.930(2)	23.674(6)
α (deg)	89.367(6)	90.00
β (deg)	74.859(6)	90.00
γ (deg)	75.365(6)	90.00
Volume (Å^3)	1984.5(5)	7516(3)
Z	2	8
D_{calc} (Mg m^{-3})	1.637	1.661
Absorption coefficient (mm^{-1})	2.196	1.962
F(000)	982	3776
Crystal size (mm)	0.38 × 0.35 × 0.29	0.38 × 0.34 × 0.30
θ range for data collection (deg)	1.52–26.00	2.36–27.65
Index ranges	$-14 \le h \le 14$, $-15 \le k \le 16$, $-16 \le l \le 17$	$-22 \le h \le 23$, $-23 \le k \le 20$, $-29 \le l \le 29$
Reflections collected	7710	6008
Independent reflections(R_{int})	6712(0.0566)	8836(0.0518)
Data/restraints/parameters	7710/0/466	8836/6/531
Absorption correction	Semi-empirical from equivalents	Semi-empirical from equivalents
Refinement method	Full-matrix least-squares on F^2	Full-matrix least-squares on F^2
Goodness-of-fit on F^2	1.080	1.002
R indices (all data)	R_1=0.0408, wR_2=0.1079	R_1=0.0604, wR_2=0.0727
Final R indices [I > 2σ(I)]	R_1=0.0468, wR_2=0.1121	R_1=0.0304, wR_2=0.0613

Table 2
Selected bond lengths (Å) and angles (deg) for the complex $[ErL^{I}(NO_3)_3(CH_3CO_2Et)]_n$.

Er(1)–O(5)	2.286(2)	Er(1)–O(2)	2.291(2)	Er(1)–O(16)	2.366(3)
Er(1)–O(13)	2.398(3)	Er(1)–O(9)	2.414(3)	Er(1)–O(10)	2.426(3)
Er(1)–O(15)	2.431(3)	Er(1)–O(12)	2.442(3)	Er(1)–O(7)	2.447(3)
O(5)–Er(1)–O(2)	86.77(9)	O(5)–Er(1)–O(16)	148.76(10)	O(2)–Er(1)–O(13)	125.31(10)
O(16)–Er(1)–O(13)	75.71(10)	O(5)–Er(1)–O(9)	81.64(10)	O(2)–Er(1)–O(9)	81.49(10)
O(5)–Er(1)–O(10)	126.84(9)	O(2)–Er(1)–O(10)	141.32(9)	O(16)–Er(1)–O(10)	71.74(10)
O(13)–Er(1)–O(10)	82.69(10)	O(9)–Er(1)–O(10)	85.02(11)	O(5)–Er(1)–O(15)	77.05(9)
O(2)–Er(1)–O(15)	72.63(9)	O(16)–Er(1)–O(15)	72.11(9)	O(13)–Er(1)–O(15)	52.69(9)
O(9)–Er(1)–O(15)	147.11(11)	O(10)–Er(1)–O(15)	127.86(10)	O(5)–Er(1)–O(12)	75.34(9)
O(2)–Er(1)–O(12)	151.14(10)	O(16)–Er(1)–O(12)	118.21(10)	O(13)–Er(1)–O(12)	74.96(11)
O(9)–Er(1)–O(12)	73.73(11)	O(10)–Er(1)–O(12)	51.53(9)	O(15)–Er(1)–O(12)	123.28(10)
O(5)–Er(1)–O(7)	130.71(10)	O(2)–Er(1)–O(7)	71.44(10)	O(16)–Er(1)–O(7)	76.17(10)
O(13)–Er(1)–O(7)	146.59(11)	O(9)–Er(1)–O(7)	52.37(10)	O(10)–Er(1)–O(7)	71.61(11)
O(15)–Er(1)–O(7)	131.90(10)	O(12)–Er(1)–O(7)	103.33(11)		

Table 3
Selected bond lengths (Å) and angles (deg) for the complex $\{[TbL^{II}(NO_3)_3(H_2O)]\cdot(H_2O)\}_n$.

Tb(1)–O(1)	2.486(2)	Tb(1)–O(2)	2.460(2)	Tb(1)–O(3)	2.465(2)
Tb(1)–O(4)	2.524(3)	Tb(1)–O(7)	2.486(2)	Tb(1)–O(10)	2.475(2)
Tb(1)–O(11)	2.334(2)	Tb(1)–O(13)	2.314(2)	Tb(1)–O(17)	2.310(2)
O(17)–Tb(1)–O(13)	86.34(9)	O(17)–Tb(1)–O(11)	80.23(8)	O(13)–Tb(1)–O(11)	83.36(8)
O(17)–Tb(1)–O(2)	83.98(8)	O(13)–Tb(1)–O(2)	148.82(8)	O(11)–Tb(1)–O(2)	123.74(8)
O(17)–Tb(1)–O(3)	155.80(8)	O(13)–Tb(1)–O(3)	77.60(8)	O(11)–Tb(1)–O(3)	80.02(8)
O(2)–Tb(1)–O(3)	118.83(8)	O(17)–Tb(1)–O(10)	125.21(10)	O(13)–Tb(1)–O(10)	82.29(9)
O(11)–Tb(1)–O(10)	149.62(9)	O(2)–Tb(1)–O(10)	79.34(9)	O(3)–Tb(1)–O(10)	70.81(9)
O(17)–Tb(1)–O(1)	81.41(8)	O(13)–Tb(1)–O(1)	154.68(8)	O(11)–Tb(1)–O(1)	72.79(8)
O(2)–Tb(1)–O(1)	51.52(7)	O(3)–Tb(1)–O(1)	105.79(8)	O(10)–Tb(1)–O(1)	122.80(8)
O(17)–Tb(1)–O(7)	74.09(9)	O(13)–Tb(1)–O(7)	75.23(9)	O(11)–Tb(1)–O(7)	147.31(8)
O(2)–Tb(1)–O(7)	73.61(8)	O(3)–Tb(1)–O(7)	118.01(9)	O(10)–Tb(1)–O(7)	51.16(10)
O(1)–Tb(1)–O(7)	121.69(8)	O(17)–Tb(1)–O(4)	147.31(9)	O(13)–Tb(1)–O(4)	126.29(9)
O(11)–Tb(1)–O(4)	99.79(9)	O(2)–Tb(1)–O(4)	68.72(8)	O(3)–Tb(1)–O(4)	51.00(8)
O(10)–Tb(1)–O(4)	68.35(10)	O(1)–Tb(1)–O(4)	67.72(9)	O(7)–Tb(1)–O(4)	112.76(9)

The podand 1,2-bis{[2'-(2-pyridylmethylaminoformyl)phenoxyl]methyl}benzene (L^{II}) was synthesized and characterized as reported in our previous paper [20].

2.5. Syntheses of the complexes

The 0.1 mmol lanthanide nitrate (*Ln*=Gd, Tb, Er) was dissolved in 5 cm^3 of ethyl acetate, then the solution of 0.1 mmol ligand L^{I} in 5 cm^3 of ethyl acetate was added dropwise. The mixture was stirred at room temperature for 4 h. And then the precipitated solid complex was filtered, washed with ethyl acetate, dried in vacuum over P_4O_{10} for 48 h and submitted for elemental analysis.

$[GdL^{I}(NO_3)_3]\cdot CH_3CO_2Et$ yield 67%. Anal. Calcd for $C_{36}H_{36}N_5O_{17}Gd$ (%): C, 44.67; H, 3.75; N, 7.24; Found (%): C, 44.72; H, 3.64; N, 7.55. Major IR bands (KBr; cm^{-1}), ν(C=O): 1617, $\nu_1(NO_3^-)$: 1503, $\nu_4(NO_3^-)$: 1296, $\nu_2(NO_3^-)$: 1028, $\nu_5(NO_3^-)$: 815, ν(C=O ethyl acetate): 1681. $[TbL^{I}(NO_3)_3]\cdot CH_3CO_2Et$ yield 70%. Anal. Calcd for $C_{36}H_{36}N_5O_{17}Tb$ (%): C, 44.59; H, 3.74; N, 7.22; Found (%): C, 44.89; H, 3.71; N, 7.33. Major IR bands (KBr; cm^{-1}), ν(C=O): 1618, $\nu_1(NO_3^-)$: 1504, $\nu_4(NO_3^-)$: 1297, $\nu_2(NO_3^-)$: 1028, $\nu_5(NO_3^-)$: 815, ν(C=O ethyl acetate): 1681. $[ErL^{I-}(NO_3)_3]\cdot CH_3CO_2Et$ yield 61%. Anal. Calcd. for $C_{36}H_{36}N_5O_{17}Er$ (%): C, 44.21; H, 3.71; N, 7.16; Found (%): C, 44.28; H, 3.56; N, 7.21. Major IR bands (KBr; cm^{-1}), ν(C=O): 1620, $\nu_1(NO_3^-)$: 1507, $\nu_4(NO_3^-)$: 1299, $\nu_2(NO_3^-)$: 1029, $\nu_5(NO_3^-)$: 815, ν(C=O ethyl acetate): 1682.

General procedure for the synthesis of lanthanide complexes $[TbL^{II}(NO_3)_3]\cdot 2H_2O$ and $[GdL^{II}(NO_3)_3]\cdot 2H_2O$, the elemental analyses and IR spectra characterization of the complexes were reported before [20].

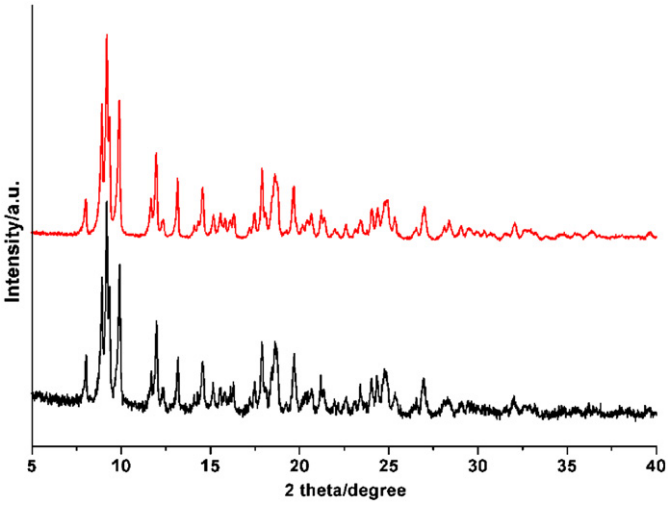

Fig. 1. The powder X-ray diffraction patterns for Tb (upper) and Er (lower) complexes with the ligand L^{I}.

3. Results and discussion

3.1. Physical measurements

The new complexes gave satisfactory microanalytical results, justifying their purity. Analytical data for the complexes with the ligand L^{I} conform to a 1:1 (metal:L) stoichiometry $[LnL^{I}(NO_3)_3]\cdot CH_3CO_2Et$ (*Ln*=Gd, Tb, Er). All the complexes are soluble in DMF,

DMSO, methanol, ethanol, acetone, but slightly soluble in acetonitrile, THF and ethyl ether.

The complexes have the similar powder X-ray diffraction patterns and IR spectra, of which the characteristic bands have similar shifts, suggesting that they have a similar coordination structure.

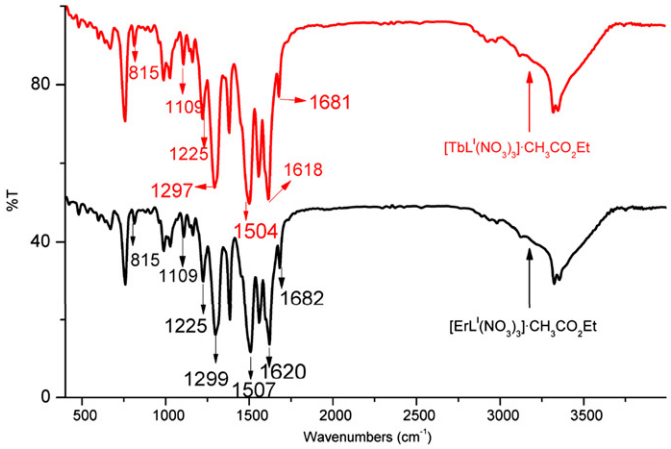

Fig. 2. The IR spectra of Tb (upper) and Er (lower) complexes with the ligand L^I.

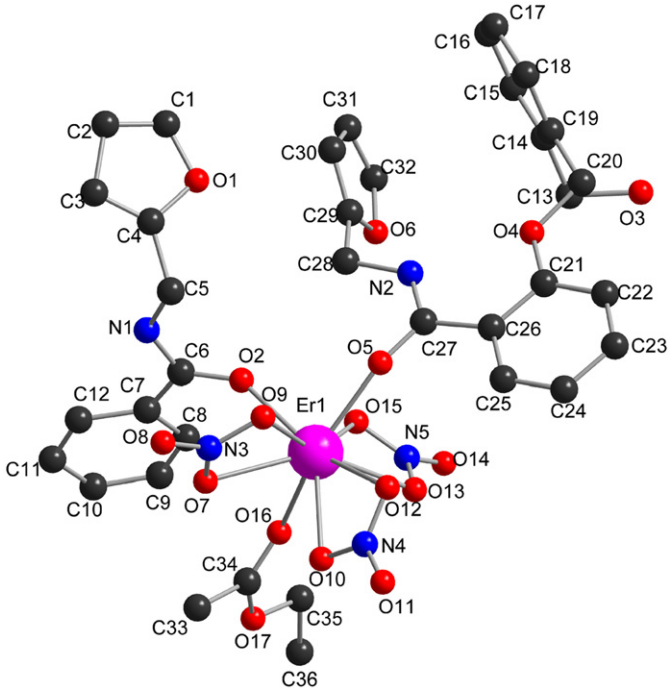

Fig. 3. Structure of $[ErL^I(NO_3)_3(CH_3CO_2Et)]_n$ showing the coordination sphere of Er^{3+} along with atom labeling schemes (hydrogen atoms are omitted for clarity).

The room temperature PXRD patterns of the Tb(III) and Er(III) complexes with the ligand L^I are unfolded from 5° to 40° as shown in Fig. 1, and the IR spectra of the complexes are presented in Fig. 2.

The characteristic bands of the ν(C=O), ν(C–O–C) of free ligand L^I are shown at 1639 and 1115 cm^{-1}, respectively. In the IR spectra of the complexes, the low-energy bands remain unchanged, but the high-energy bands of the complexes red shift to about 1618 cm^{-1} ($\Delta\nu$=21 cm^{-1}) as compared to the free ligand, thus indicating that only the oxygen atoms of C=O take part in coordination to the lanthanide ions. The band at about 1681 cm^{-1} may be assigned to the ν(C=O) of the ethyl acetate molecules. The absorption bands of complexes assigned to the coordinated nitrate groups (C_{2v}) are observed at about 1503 cm^{-1} (ν_1), 1296 cm^{-1} (ν_4), 1028 cm^{-1} (ν_2) and 815 cm^{-1} (ν_5) [23]. The separation of two strongest frequency bands $|\nu_1-\nu_4|$ lies at about 200 cm^{-1}, clearly establishing that the NO_3^- groups in the solid complexes coordinate to the lanthanide ions as bidentate ligands [24].

3.2. Crystal structure descriptions

$[ErL^I(NO_3)_3(CH_3CO_2Et)]_n$ Pink crystals suitable for X-ray diffraction were obtained by slow evaporation of the methanol and ethyl acetate mixture (V:V=1:2) solution of the Er(III) complex. The single-crystal X-ray analysis of the complex $[ErL^I(NO_3)_3(CH_3CO_2Et)]_n$ reveals that the crystal crystallizes in triclinic $P-1$ space group and each Er^{3+} is coordinated with nine oxygen donor atoms, six of which belong to three bidentate nitrate groups, two belong to carbonyl groups from two bridging podands and the remaining one to coordinated ethyl acetate molecule, with Er–O distances range from 2.286(2) to 2.447(3) Å (Fig. 3). The coordination polyhedron around the Er(III) is a distorted tricapped triprism. At the same time, each ligand binds to two Er(III) using its two oxygen atoms of the amide groups. So the whole structure consists of an infinite array of Er(III) bridged by bidentate ligands and a one-dimensional (1D) coordination polymeric linear chain is formed (Fig. 4).

Many lanthanide complexes based on the same ligand usually have alike building blocks due to similar valence shell electron configurations [25–27], thus we may deduce that the structure of Tb^{3+} complex is similar to Er^{3+} complex, which can also be proved by the PXRD patterns and IR spectra.

$\{[TbL^{II}(NO_3)_3(H_2O)]\cdot(H_2O)\}_n$ Colorless crystals suitable for X-ray diffraction were obtained by slow evaporation of the methanol and ethyl acetate mixture (V:V=1:2) solution of the Tb^{3+} complex. The single-crystal X-ray analysis of the complex $\{[TbL^{II}(NO_3)_3(H_2O)]\cdot(H_2O)\}_n$ reveals that each Tb^{3+} ion is coordinated with nine oxygen donor atoms, six of which belong to three bidentate nitrate groups, two belong to carbonyl groups from two bridging podands and the remaining one to coordinated water molecule (Fig. 5). The coordination polyhedron around Tb^{3+} is a distorted tricapped triprism. Every asymmetric unit contains one crystal water molecule. At the same time, each ligand binds to two Tb^{3+} ions using its two oxygen atoms of the amide groups. So the whole structure consists of an infinite array of Tb^{3+} ions bridged by bidentate ligands and a one-dimensional (1D) zig-zag coordination polymeric chain is formed (Fig. 6). The Tb–Tb

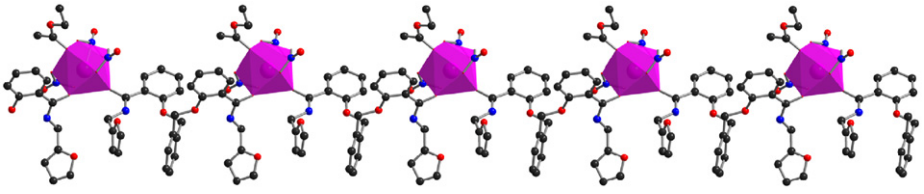

Fig. 4. 1D coordination polymer linear chain of $[ErL^I(NO_3)_3(CH_3CO_2Et)]_n$ (hydrogen atoms are omitted for clarity).

separations linked by the same bridging ligand are about 16.007 Å and the separations between alternate Tb(III) centers (on the same side of the zig-zag) are about 17.818 Å. The Tb–Tb–Tb internal angle of 67.64°. Furthermore, the zig-zag coordination chains are formed through the π–π interaction between the benzyl groups of the two arms of neighboring ligands which are almost parallel (the centroid-to-centroid distance and dihedral angle between them are 3.802 Å and 4.69°).

In the context of inorganic crystal engineering, the combination of coordination chemistry with non-covalent interactions, such as hydrogen bonding, provides a powerful method for generating supramolecular architectures from simple building blocks. The oxygen atoms of the nitrate anions and crystal water molecules (O3 and O16), the nitrogen atoms of the terminal pyridyl groups (N6) act as hydrogen bond acceptors while the oxygen atoms of the crystal and coordinated water molecules (O16 and O17) act as donors (listed in Table 4), constitute complementary hydrogen bonding recognition sites on the backbone of the 1D coordination polymer. As a result, neutral chains are interpenetrated into a 3D supramolecular structure (Fig. 7).

There were also strong intramolecular hydrogen bonding between the amide nitrogen atoms (N4 and N5) and the etheric oxygen atoms (O14 and O15), as well as the oxygen atoms of the coordinated water molecules (O17) and the nitrogen atoms of terminal pyridyl groups (listed in Table 4) within Tb(III) complex. It is no doubt to note that the robust intramolecular hydrogen bond have a template effect and participate in the stabilization of the complete architecture.

3.3. Luminescent properties of the complexes

Monitored by the emission band at 545 or 543 nm, the Tb(III) complexes $[TbL^{I}(NO_3)_3(CH_3CO_2Et)]_n$ and $\{[TbL^{II}(NO_3)_3(H_2O)]\cdot(H_2O)\}_n$ both exhibit broad excitation bands around 320 nm. The luminescence emission spectra of these two Tb(III) complexes in solid state (the excitation and emission slit widths were 1.0 nm (Fig. 8)) were recorded at room temperature. It can be seen from Fig. 8 that the complexes show the characteristic *f*–*f* transition emissions of Tb(III) when excited with 321 and 322 nm, respectively, in the solid state (the data listed in Table 5). These indicate

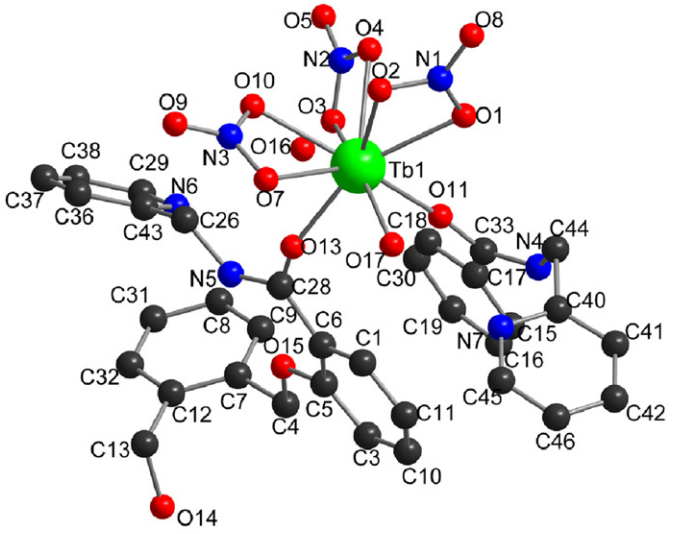

Fig. 5. Structure of $\{[TbL^{II}(NO_3)_3(H_2O)]\cdot(H_2O)\}_n$ showing the coordination sphere of Tb^{3+} along with atom labeling schemes (hydrogen atoms and crystalline water molecule are omitted for clarity).

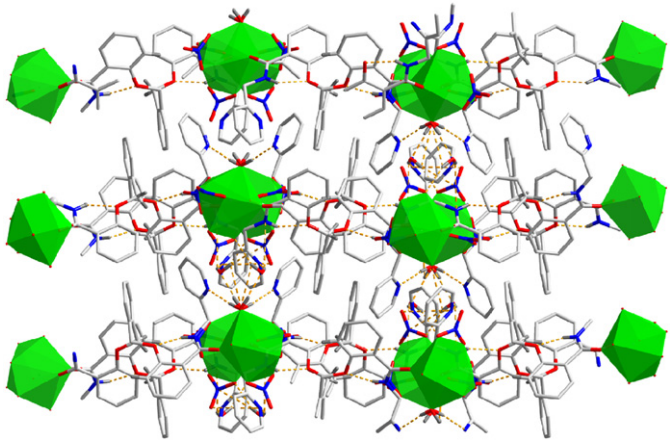

Fig. 7. The 3D supramolecular structure of $\{[TbL^{II}(NO_3)_3(H_2O)]\cdot(H_2O)\}_n$ constructed by hydrogen bonds. (The nitrate anions without formed hydrogen bonds are omitted for clarity.)

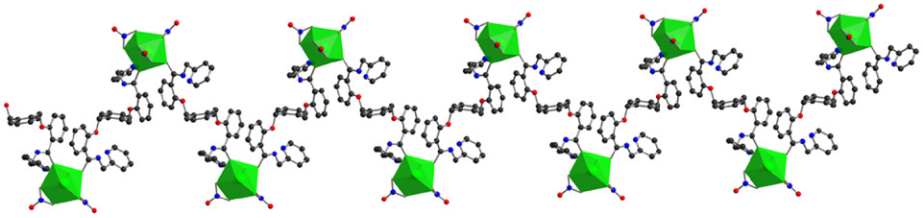

Fig. 6. 1D zig-zag coordination polymer of $\{[TbL^{II}(NO_3)_3(H_2O)]\cdot(H_2O)\}_n$ (hydrogen atoms and crystalline water molecules are omitted for clarity).

Table 4
Hydrogen bonds in crystal packing (Å, deg) of $\{[TbL^{II}(NO_3)_3(H_2O)]\cdot(H_2O)\}_n$.

D–H···A	*d*(D–H)	*d*(H···A)	*d*(D···A)	∠DHA	Symmetry code
O(16)–H(16C)···N(6) (inter)	0.86	2.01	2.8350	160	
O(16)–H(16D)···O(3) (inter)	0.86	2.04	2.8757	164	
O(17)–H(17D)···O(16) (inter)	0.87	1.78	2.6353	167	$-x, -1/2+y, 1/2-z$
N(4)–H(4)···O(14) (intra)	0.86	1.98	2.6322	132	$-1/2+x, 1/2-y, 1-z$
O(5)–H(5)···O(15) (intra)	0.86	2.01	2.6700	132	
O(17)–H(17C)···N(7) (intra)	0.84	1.95	2.7796	173	

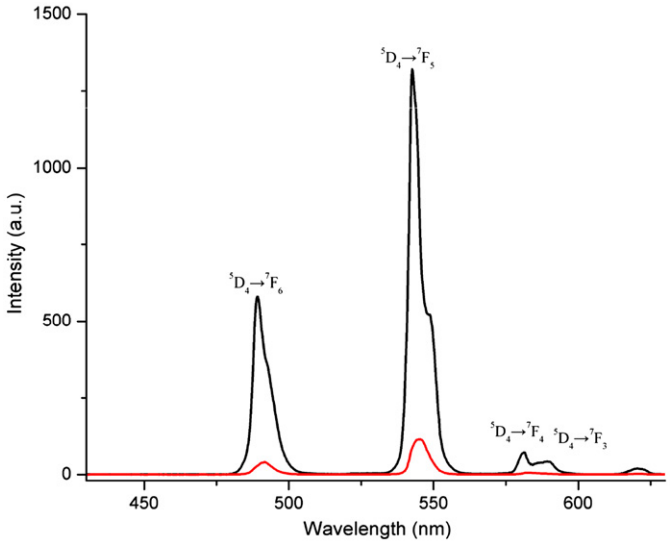

Fig. 8. Emission spectra of the Tb^{3+} complexes with the ligand L^I (weak) and L^{II} (strong).

Table 5
Luminescence data for the Tb(III) complexes in solid state at room temperature.

Complexes	λ_{Ex} (nm)	λ_{Em} (nm)	RFI[a]	Assignments
$[TbL^I(NO_3)_3(CH_3CO_2Et)]_n$	321	492	40	$^5D_4 \rightarrow {}^7F_6$
		545	116	$^5D_4 \rightarrow {}^7F_5$
		583	6	$^5D_4 \rightarrow {}^7F_4$
		620	2	$^5D_4 \rightarrow {}^7F_3$
$\{[TbL^{II}(NO_3)_3(H_2O)] \cdot H_2O\}_n$	322	489	581	$^5D_4 \rightarrow {}^7F_6$
		543	1321	$^5D_4 \rightarrow {}^7F_5$
		581	72	$^5D_4 \rightarrow {}^7F_4$
		620	21	$^5D_4 \rightarrow {}^7F_3$

[a] RFI: relative luminescence intensity.

that the ligands L^I and L^{II} are comparatively good organic chelators to absorb and transfer the energy to the central Tb^{3+} ions.

An intramolecular energy transfer from the triplet state of the ligand to the resonance level of the Ln(III) ion is one of the most important process having influence on the Ln(III) luminescent properties of Ln(III) chelates [28]. A triplet excited state T_1 which is localized on one ligand only and is independent of the nature of the lanthanide ions [28]. The triplet state energy levels T_1 of the ligands L^I and L^{II}, which were calculated from the shortest-wavelength phosphorescence bands [28], are 24,449 and 24,814 cm^{-1} [20]. These energy levels are both above the lowest excited resonance level $^5D_4$ (20,545 cm^{-1}) of Tb(III). Thus, the absorbed energy could be transferred from ligands to the Tb^{3+} ions.

The fluorescence quantum yield Φ of the complex $\{[TbL^{II}(NO_3)_3(H_2O)] \cdot H_2O\}_n$ in solid state was found to be $41.1 \pm 0.1\%$ using an integrating sphere, which is higher than the complex $[TbL^I(NO_3)_3(CH_3CO_2Et)]_n$ ($28.8 \pm 0.1\%$). And the luminescence decay of the two Tb(III) complexes are best described by a single-exponential process with significantly longer lifetimes of $\tau = 1.425 \pm 0.001$ ms ($\{[TbL^{II}(NO_3)_3(H_2O)] \cdot H_2O\}_n$) and $\tau = 1.372 \pm 0.001$ ms ($[TbL^I(NO_3)_3(CH_3CO_2Et)]_n$), indicating the presence of one distinct emitting species, respectively. From the crystal structures of the complexes, we could find that the coordination environments of the Tb^{3+} ions are similar with the two ligands L^I and L^{II}, but the luminescent properties of the L^{II} complex which contain coordinated water and crystal water is greatly better than the L^I complex without water molecule. It is well-known that the O–H oscillator of the solvent coordinated to the metal center can provide an efficient nonradiative path [29,30]. On the basis of the crystal structure analysis, we may deduce that the nonradiative transitions due to the O–H oscillators and the vibration of the ligands in the Tb(III) first coordination shell of the L^{II} complex, which may quench the luminescence of the central ions, were weakened and restrained to some extent by the hydrogen bonding interactions between the coordinated water molecule, the terminal picolyl group and the crystallized water molecules, thus bringing the excellent luminescence efficiency of the hydrated L^{II} complex.

4. Conclusion

This study demonstrates that two structure-related bridging podands with terminal groups from furan to pyridine of salicylamide, 1,2-bis{[(2'-furfurylaminoformyl)phenoxyl]methyl}benzene (L^I) and 1,2-bis{[2'-(2-pyridylmethylaminoformyl)phenoxyl]methyl}benzene (L^{II}), form 1D linear chain and zig-zag coordination polymers $[ErL^I(NO_3)_3(CH_3CO_2Et)]_n$ and $\{[TbL^{II}(NO_3)_3(H_2O)] \cdot (H_2O)\}_n$ with lanthanide cations via the carbonyl oxygen donors. In $\{[TbL^{II}(NO_3)_3(H_2O)] \cdot (H_2O)\}_n$, the free and coordinated water molecules play an important role in the structure, which links the neutral chains with two hydrogen bonds from two different directions, as a result, the neutral chains are interpenetrated into a 3D supramolecular structure. The luminescent properties of the Tb(III) complexes in solid state were investigated. And the lowest triplet state energy levels of the podands L^I and L^{II} indicate that the antennae with different terminal groups are both good organic chelators to absorb energy and transfer them to central Tb^{3+} ions. The complex $\{[TbL^{II}(NO_3)_3(H_2O)] \cdot (H_2O)\}_n$ which contains coordinated and crystal water molecules displays better fluorescence quantum yield and longer lifetime than the L^I complex $[TbL^I(NO_3)_3(CH_3CO_2Et)]_n$. This phenomenon may be produced by that the nonradiative transitions due to the O–H oscillators and the vibration of the ligands in the Tb(III) first coordination shell of the L^{II} complex were restrained to some extent by the hydrogen bonding interactions.

Supplementary material

Crystallographic data for the structural analysis have been deposited with the Cambridge Crystallographic Data Center, CCDC nos. 783278 and 783279. Copies of this information may be obtained free of charge from the director, CCDC, 12 Union Road, Cambridge CB2 IEZ, UK (e-mail: deposit@ccdc.cam.ac.uk or www: http://www.ccdc.cam.ac.uk).

Acknowledgments

This work was supported by the National Natural Science Foundation of China (Project No. 20931003) and the program for New Century Excellent Talents in University (NCET-06-0902).

Appendix A. Supplementary material

Supplementary data associated with this article can be found in the online version at doi:10.1016/j.jssc.2010.11.011.

References

[1] F.L. Zhang, Y.H. Hou, C.X. Du, Y.J. Wu, Dalton Trans. (2009) 7359.
[2] C.M.G. Santos, A.J. Harte, S.J. Quinn, T. Gunnlaugsson, Coord. Chem. Rev. 252 (2008) 2512.

[3] L. Armelao, S. Quici, F. Barigelletti, G. Accorsi, G. Bottaro, M. Cavazzini, E. Tondello, Coord. Chem. Rev. 254 (2010) 487.
[4] J.P. Leonard, C.M.G. Santos, S.E. Plush, T. McCabe, T. Gunnlaugsson, Chem. Commun. (2007) 129.
[5] J.M. Lehn, Angew. Chem. Int. Ed. 29 (1990) 1304.
[6] S. Ida, C. Ogata, D. Shiga, K. Izawa, K. Ikeue, Y. Matsumoto, Angew. Chem. Int. Ed. 47 (2008) 2480.
[7] J.P. Leonard, P. Jensen, T. McCabe, J.E. O'Brien, R.D. Peacock, P.E. Kruger, T. Gunnlaugsson, J. Am. Chem. Soc. 129 (2007) 10986.
[8] M. Jiang, X. Zhai, M. Liu, Langmuir 21 (2005) 11128.
[9] A. Gulino, F. Lupo, G.G. Condorelli, A. Motta, I.L. Fragalà, J. Mater. Chem. 19 (2009) 3507.
[10] D.B.A. Raj, S. Biju, M.L.P. Reddy, Dalton Trans. (2009) 7519.
[11] H. Heil, J. Steiger, R. Schmechel, H.V. Seggern, J. Appl. Phys. 90 (2001) 5357.
[12] E.G. Moore, A.P.S. Samuel, K.N. Raymond, Acc. Chem. Res. 42 (2009) 542.
[13] S. Petoud, S.M. Cohen, J.-C.G. Bünzli, K.N. Raymond, J. Am. Chem. Soc. 125 (2003) 13324.
[14] J.-C.G. Bünzli, Acc. Chem. Res. 39 (2006) 53.
[15] J.-M. Lehn, Angew. Chem. Int. Ed. 29 (1990) 1304.
[16] N. Sabbatini, M. Guardigli, J.-M. Lehn, Coord. Chem. Rev. 123 (1993) 201.
[17] J.-C.G. Bünzli, C. Piguet, Chem. Soc. Rev. 34 (2005) 1048.
[18] X.-Q. Song, W.-S. Liu, W. Dou, J.-R. Zheng, X.-L. Tang, H.-R. Zhang, D.-Q. Wang, Dalton Trans. (2008) 3582.
[19] C. Bazzicalupi, A. Bencini, A. Bianchi, C. Ciorgi, V. Fusi, A.M.B. Valtancoli, A. Roque, F. Pina, Chem. Commun. 7 (2000) 561.
[20] Q. Wang, X.-H. Yan, W.-S. Liu, M.-Y. Tan, Y. Tang, J. Fluoresc. 20 (2010) 493.
[21] Z. Jiri, P. Magdalena, H. Petr, T. Milos, Synthese 110 (1994) 1132.
[22] G.M. Sheldrick, SHELXS-97, A Program for X-ray Crystal Structure Solution, and SHELXL-97, A Program for X-ray Structure Refinement, Gottingén University, Germany, 1997.
[23] W. Carnall, S. Siegel, J. Ferrano, B. Tani, E. Gebert, Inorg. Chem. 12 (1973) 560.
[24] K. Nakamoto, Infrared and Raman Spectra of Inorganic and Coordination Compounds, 4th ed, John Wiley, New York, 1978.
[25] J.-R. Li, X.-H. Bu, R.-H. Zhang, C.-Y. Duan, K.M.-C. Wong, V.W.-W. Yam, New J. Chem. 28 (2004) 261.
[26] G.M. Davies, R.J. Aarons, G.R. Motson, J.C. Jeffery, H. Adams, S. Faulkner, M.D. Ward, Dalton Trans. (2004) 1136.
[27] B.D. Chandler, D.T. Cramb, G.K.H. Shimizu, J. Am. Chem. Soc. 128 (2006) 10403.
[28] M. Latva, H. Takalob, V.M. Mukkala, C. Matachescuc, J.C. Rodriguez-Ubisd, J. Kankarea, J. Lumin. 75 (1997) 149.
[29] W.D.J. Horrocks, D.R. Sudnick, Acc. Chem. Res. 14 (1981) 384.
[30] Y.L. Guo, W. Dou, X.Y. Zhou, W.S. Liu, W.W. Qin, Z.P. Zang, H.R. Zhang, D.Q. Wang, Inorg. Chem. 48 (2009) 3581.